All Sciences Proceedings

1st International Conference on Recent and Innovative Results in Engineering and Technology

August 16-18, 2023 : Konya, Turkey

ICRIRET

All Sciences Proceedings
http://as-proceeding.com/

© 2023 Published by All Sciences Proceedings

https://as-proceeding.com/index.php/icriret

CZTS/ZnS solar cell modelled with SCAPS-1D simulation program

Serap YIGIT GEZGIN[1], Silan BATURAY[2], Hamdi Sukur KILIC[1,3,4]

[1]*Department of Physics, Faculty of Science, University of Selcuk, 42031 Selcuklu, Konya, Turkey*
[2]*Department of Physics, Faculty of Science, Dicle University, 21280 Diyarbakir, Turkey*
[3]*Directorate of High Technology Research and Application Center, University of Selcuk, 42031 Selcuklu, Konya, Turkey*
[4]*Directorate of Laser Induced Proton Therapy Application and Research Center, University of Selçuk, 42031 Konya, Turkey*

**Corresponding author e-mail: silan@dicle.edu.tr*

Abstract – In the study, zinc sulphide (ZnS) thin films compound of the II–VI group were fabricated by known as ultrasonic spray pyrolysis technique (USP) on glass substrates. Optical properties of these films were characterized by using ultraviolet–visible (UV–Vis) spectrophotometry. Measurements of Ultraviolet–visible spectroscopy point out that the absorbance and direct band gap of zinc sulphide samples annealed at diverse ambient is improved. Energy band gap of the obtained ZnS thin film found to be 3.75, 3.66, 3.58, 3.68 and 3.70 eV for ZnS-as grown, ZnS-N_2, ZnS-air, ZnS-H_2S 500, ZnS-H_2S 550 films, respectively. ZnS thin film, which is annealed H2S:Ar ambient at 550 °C, has higher absorption and extinction coefficient compared to other thin films. Refractive indices were calculated with Moss and Herve&Vardamme relations. ZnS thin film, which is annealed at air ambient has the highest refractive index, ZnS thin film, which is not annealed has the lowest one. Au/CZTS/ZnS-500&ZnS-550/i-ZnO/AZO solar cells that is modelled by SCAPS simulation. N_D value from 2.10^{16} to 1.10^{17} cm^{-3}, V_{OC}, J_{SC} and η values, which decreased from 0.711 V to 0.576 V, from 15.44 $mAcm^{-2}$ to 10.78 $mAcm^{-2}$, from 7.48% to 4.47%, respectively. SnO_2 intermediate layer, is placed between CZTS and ZnS layers, caused more charge separation at the two interfaces and increased V_{OC} and efficiency of the solar cell.

Keywords – ZnS Thin Film, SnO_2 Intermediate, Solar Cell, SCAPS-1D

1. Introduction

Solar cells based on thin films have been seen as a key role in energy resolution due to their great conversion rates, ease of mass manufacture, and low manufacturing cost. Indium (In), gallium(Ga) selenide(Se) (CIGS), cadmium(Cd) telluride(Te) (CdTe), and copper(Cu) are among the most efficient thin-film solar cells [1]. Both bulk and thin solar cells are the two main solar cells types. Solar cells made of CdTe (Cadmium Telluride) and CIGS (CuInGa(S,Se_2)) are the most effective and have the highest uses [2]. Solar cell technologies of the thin-film based on polycrystalline absorbers, CIGS and CdTe, have attained highest efficiencies of around 23% and 22%, respectively, in laboratory devices and have already reached the commercial manufacturing stage [3, 4]. As buffer layers in these solar cells, CdS thin films are utilized [5, 6]. Since cadmium is toxic and causes serious damage to living things, it is not an environmentally friendly material. The process of recycling equipment using a toxic component that will negatively impact the environment does not make sense in an eco-friendly project. Therefore, it is vital to seek a non-toxic element that is good for both environmental and industrial level production. As a result of using thin films based on un doped ZnO or doped ZnO as TCO, non-doped ZnS film as the buffer layer, and Cu_2ZnSnS_4 as the absorbent layer to produce a suitable heterostructure enables us to gain a solar cell with abundant and environmentally friendly material [7, 8].

Furthermore, these aren't abundant on earth, but they are expensive. CZTS is the most cost-effective and environmentally friendly absorber layer for solar cells, due to its richness in the earth's crust and

eco-friendliness. The Cu_2ZnSnS_4 solar cell has the likely to be a low manufacturing cost, high-efficiency rates of solar power [9]. Its components are non-toxic and these have been gained much plentiful in earth's crust [10, 11]. Solar cell absorber layers made from CZTS are among the most promising materials because of their outstanding optical properties (band gaps between 1.4 and 1.5 eV and absorption coefficients exceeding 10^4 cm^{-1} [12, 13]. Nanocrystalline ZnS film can crystallize in three different crystallize form such as sphalerite structure, cubic structure [14] which is very stable at room temperature and a hexagonal form with wurtzite structure which is stable at 1020 °C and above at atmospheric pressure [15, 16]. Nanocrystalline ZnS has a rather wide energy band gap of 3.5 and 3.9 eV and a high index of refractive (2-2.5) with high transmittance value in both the visible and infrared regions [17-19]. Zinc sulfide displays a number of intriguing benefits when acting as a buffer layer between the absorbent layer and the TCO (ZnO: Al), including lowering absorbent/TCO band shifts and offering efficient photogenerated carrier separation. The use of ZnS film as a buffer between the absorbent layer and the TCO (ZnO: Al) layer has a number of intriguing benefits, including lowering the absorbent/TCO band shift, ensuring proper band alignment for the separation of photogenerated carriers [20] preventing interfacial distortions and defects brought on by lattice shifting between the CZTS absorber and the TCO (AZO) layer, and improving short-wavelength response [7].

In general, CdS is popularly used material as window and 'buffer layer' in solar cell [21, 22], Particular interest has been focused on improving Cd-free absorber layers in solar cells because of the toxic problem with depositing CdS buffer layers. Therefore, ZnS films have significantly been studied in recent years compared to their bulk counter parts. In this study, ZnS films were grown by using USP technique at 350°C temperature. Then, ZnS films were annealed at H_2S ambient to develop their properties. The annealed effect with different temperatures (500 ºC and 550 oC) were comprehensively investigated but the optical, structural and photovoltaic parameters using SCAPS program of the films in different annealing temperature in H2S ambient were not comprehensively investigated. Therefore, we report the structural, optical properties of ZnS films in different annealing ambient that are prepared by USP. Here, we investigated the effect of electron density, and defect density on the zinc sulphide buffer layer and the cell's performance and used zinc sulfide as the buffer layer and CZTS as the absorber layer. The SCAPS 3302 environment. was used to implement a CZTS solar cell composed of Mo/*p*-CZTS/ZnS-500&ZnS-550/I-ZnO/AZO. As a default, the illumination spectrum and operation temperature were fixed to the global AM1.5 standard and 300 K, respectively.

1. Experimental

The deposition of ZnS thin films were first prepared on soda lime glass (SLG) substrate using ultrasonic spray pyrolysis (USP) method at N_2 atmosphere. Before deposition, all SLG substrates were carefully cleaned to ensure high-quality homogenous ZnS thin films. Five steps were used for substrate cleaning procedure: firstly, substrates were heated in a mixture of 5:1:1 H_2O, NH_3, and H_2O_2 for 20 min at 95 °C, secondly, in 5:1:1 H_2O, H_2O_2, and HCl for 20 min at 95 °C. Then, ultrasonicated in ethanol for 5 min and after then, the cleaned substrates were bathed in distilled water for 5 min. and finally dried in N_2 gas to remove water on the surface of SLG substrates. A stoichiometric amount of 0.1 M zinc acetate ($Zn(CH_3COO)_2$), 0.2 M thiourea ($SC(NH_2)_2$ in deionized water were used to make ZnS thin films owing to the friendliest solvent. Thiourea is very volatile nature at high temperatures [23]. As a result, this component was added twice to avoid sulphur loss. The chemical with a 1:1 stoichiometric ratio was separately prepared in a mixture of 30 ml deionized water, a small amount of diethanolamine to regulate the pH value and mixed for 2 h on a magnetic stirrer at room temperature. During the preparation zinc acetate solution was added to the thiourea solution. After stirring for solution for 7 hours at 25 °C, the solution of ZnS became white and homogenous. The obtained ZnS solution was atomized using ultrasonic nebulizer (SonoTek Exacta-Coat) onto SLG with a frequency of 125 kHz. The solution of ZnS was sprayed using ultrasonic spray pyrolysis (USP) onto soda lime glass (SLG) heated at around 350 °C at continuously fixed nozzle–substrate separation of 9.5 cm. The fixed nozzle was operated constantly at around 125 kHz for the period of spraying process, providing median drop diameter of 8 lm. 60 cc of prepared

solution was sprayed onto SLG substrates during 50 min. The solution flow rate was kept 1 mL/min and controlled via flow meter, transported by N_2 gas to the substrate to prevent the formation of oxide. Obtained samples were annealed at 500 °C in air, 500 °C in N_2, and H_2S:Ar (1:10) at 500 °C and 550 °C for 60 min in a quartz furnace, respectively to investigate the different annealed effect.

The direct band gap as well as absorbance of the thin films was calculated in UV-Vis spectrophotometer in the wavelength range of 300–1100 nm at room temperature under air atmosphere as reference. İn our study, we will use zinc sulfide (ZnS) as absorber layer and cadmium sulfide (CdS) as buffer layer. The main subject of this simulation is to understand the viability of the material for absorber layer on CdS for buffer layer. ZnS thin-film solar cell with the structure of Mo/*p*-CZTS/ZnS-500&ZnS-550/I-ZnO/AZO was implemented in the SCAPS 1-D simulation program.

2. Discussion

2.1. The optical feature of ZnS thin films

Many factors can affect the absorbance and transmittance of nanostructured materials, such as the deposition technique, surface topology, and some deposition conditions (temperature, film thickness, annealed time). UV–Vis data obtained between 1100 and 300 nm wavelengths was used to analyse the absorbance wavelengths of ZnS thin films at room temperature. In this study, optical properties (absorption, refractive index and energy band value) of ZnS thin films were evaluated depending on the annealed parameters using the USP technique. Nanostructured thin films are analysed based on their absorption coefficients, which provide additional information about electron levels in the high-energy range of the absorption spectrum, as well as the vibrations of the atoms at low energies [24]. The absorption and energy bang gap spectrum of thin film are shown in Figure 1(a-b). As shown in Figure 1a, ZnS-H_2S 500 thin film exhibits more strong absorption than all other thin films in the all-region because of the fact that the sulfur flux rate may also induce a change in absorbance value. As a result of these absorption spectra, it was seen that ZnS-H_2S 500 film has the highest absorption value, while ZnS-As grown has the lowest. These findings demonstrate that the all samples have sensitive to absorption in the UV-vis range. A change in absorption values shows that the thin films can be used for many optical applications, including optical windows and UV filters. The energy band value of the obtained ZnS thin films can be calculated using the following equation

$$\alpha h\nu = A(h\nu - E_g)^n \quad (1)$$

Here, A material's constant, According to the nature of the transition, n = 1/2, 2, 3/2, or 3 for direct, nondirect allowed transitions, prohibited direct transitions, or forbidden nondirect transitions, respectively. $h\nu$ photon energy, E_g direct band gap and α is the absorption coefficient and it is calculated with the relation $\alpha = 4\pi k/\lambda$. E_g value is calculated from plot of $\alpha h\nu^2$versus photon energy ($h\nu$) for the obtained samples. The energy band gap values of the samples depending on the annealed atmosphere indicated in Figure 1b. The E_g value is calculated to be 3.75, 3.66, 3.58, 3.68 and 3.70 eV for ZnS-As grown, ZnS-N2, ZnS-Air, ZnS-H2S 500, ZnS-H2S 550 films, respectively. ZnS film with H_2S at 500 °C has clearly a larger optical band gaps than other films, which indicates that ZnS film could be used to regulate the optical band gap of ZnS films. The variation in the energy band gap value might be due to a difference in the thin film's crystallinity natüre. The change of energy band gap values was due to the effect of the change of crystalline quality and annealed atmosphere in the obtained films. The energy band values were different from the previous study of 3.88 eV at 30 °C to 3.75 eV at 90 °C because of the increased particle size [9] . Chabou et al. [25] indicated that the measured energy band was found to be in upon the fabrication time using chemical bath deposition method. The experimental results presented in this paper suggest that annealed atmosphere could change the physical properties of ZnS materials, such as their absorbance and energy band gap.

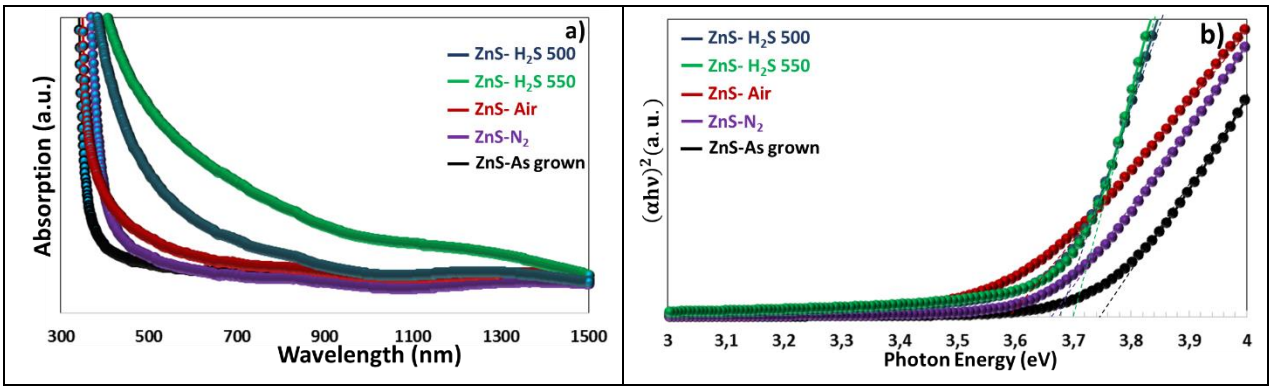

Figure 1. a) The absorption spectrum and b) the energy bands of ZnS thin films with ambients of as grown, air, N_2, H_2S at 500 ^oC and H_2S at 550 ^oC

The refractive index (n) of thin films is a parameter that affects the direction and diffusivity of light in the film. Therefore, it has an effect on the formation of photo-excited charge carriers in the thin film. The refractive indices of the samples can be found using the Moss relation expressed by Eq (2):

$$E_g n^4 = k \quad (2)$$

k, which is a constant in 108 eV. In addition, using Herve and Vandamme method, a relation can be established between E_g and n:

$$n = \sqrt{1 + \left(\frac{A}{E_g + B}\right)^2} \quad (3)$$

A and B constants, which are 13.6 eV and 3.4 eV, respectively. According to the relations expressed in equations Eq (2) and Eq (3), the refractive index decreased with the rise in the band gap [26]. In addition, these relations showed consistent results with each other [27]. Therefore, while the as grown ZnS thin film had low refractive index, the thin film annealed in air medium showed high refractive index.

3. *Determination of photovoltaic parameters of ZnS-500/CZTS and ZnS-550/CZTS solar cells using SCAPS-1D simulation program*

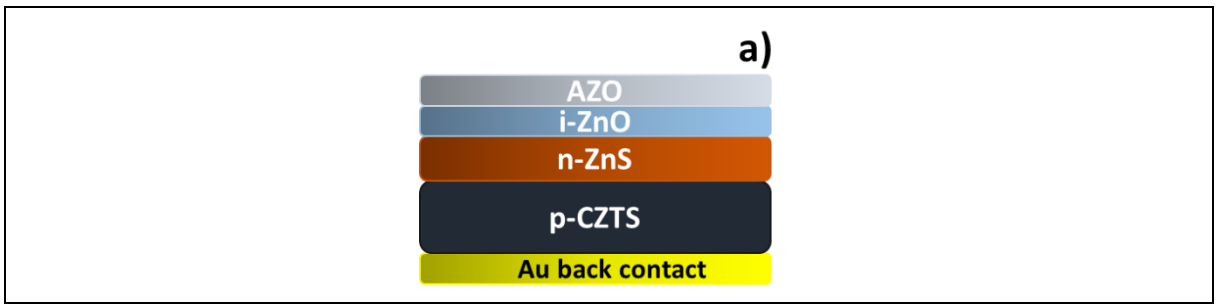

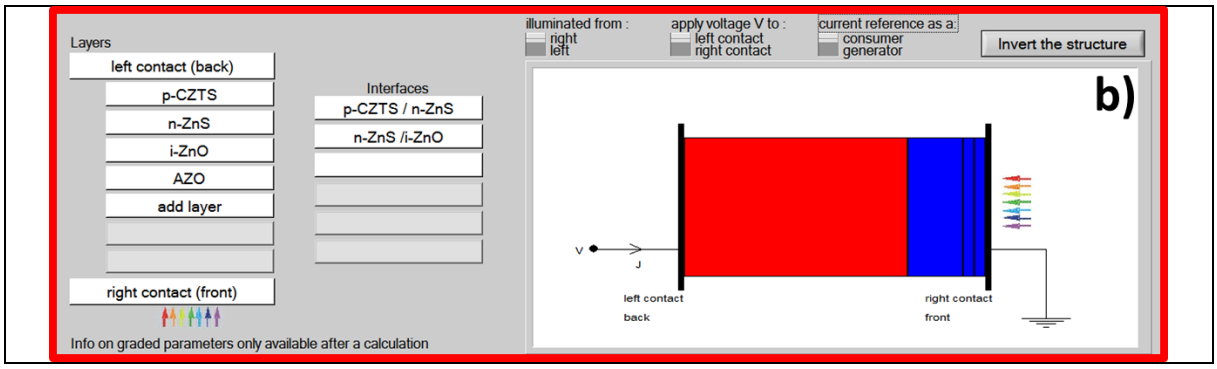

Figure 2. a) The diagram and **b)** the modelled images of ZnS/CZTS heterojunction solar cell

In this study, Mo/*p*-CZTS/ZnS-500&ZnS-550/I-ZnO/AZO solar cells were modelled and their electrical parameters were calculated by the SCAPS-1D program. If the optical and crystal properties of ZnS thin films are compared, although ZnS-500 and ZnS-550 thin films have higher photon absorption, solar cells are modelled depending on these buffer layers because they have a more advanced crystal structure in the two thin films. The parameters of the layers that make up the solar cell, which are shown in the table 1, are input to the program[28-30]. The thickness, band gap, dielectric coefficient and absorption coefficient file of the experimentally produced ZnS thin film are also uploaded to the program. The values of the other layers were taken as reference from the literature [31-33].

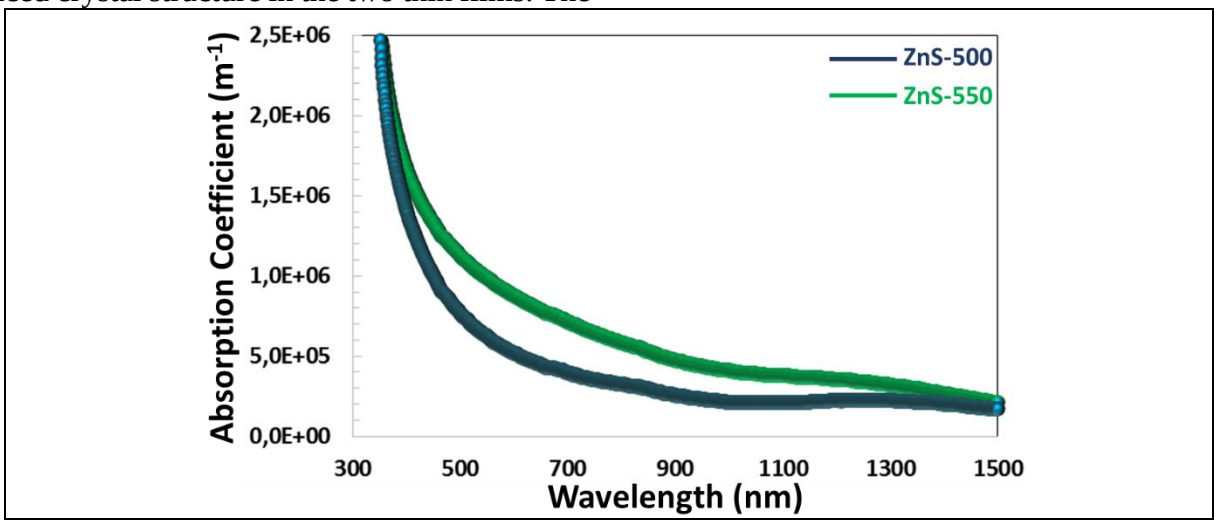

Figure 3. The absorption Coefficient spectrum of ZnS-500 and ZnS-550 thin films

According to the absorption coefficient spectrum in the Figure 3, ZnS-550 thin film has a higher absorption coefficient than that of ZnS-500 thin film in the visible-NIR wavelength regions. The formation of large particles by coalescence of small particles at higher annealing temperature that decreases the transparency of ZnS thin film somewhat. For the visible region, while the ZnS-550 thin film has an absorption coefficient between 1.66×10^{6} and 7.14×10^{5} m^{-1}, the ZnS-500 thin film indicates in 1.40×10^{6} - 3.96×10^{5} m^{-1} of absorption coefficient.

Table 1. The physical parameter of the all layer formed ZnS-500/CZTS and ZnS-550/CZTS solar cell

Layers	AZO[32]	i-ZnO[33]	ZnS-500/ZnS-550	SnO_2[34]	CZTS[31]
Band Gap (eV)	3.3	3.3	3.68/3.70	3.6	1.5
Electron affinity (eV)	4.6	4.6	3.8	4	4.50
Dielectric permittivity (relative)	9	9	7.18/7.12	9	10
CB effective density of states (cm^{-3})	$2.20x10^{18}$	$2.20x10^{18}$	$1.80x10^{18}$	$2.20x10^{18}$	$2.20x10^{18}$
VB effective density of states (cm^{-3})	$1.80x10^{19}$	$1.80x10^{19}$	$2.40x10^{19}$	$1.80x10^{19}$	$1.80x10^{20}$
Electron/Hole thermal velocity (cm/s)	$1.00x10^{7}$	$1.00x10^{7}$	$1.00x10^{7}$	$1.00x10^{7}$	$1.00x10^{7}$
Electron/Hole mobility (cm^2/Vs)	100/25	100/25	100/25	100/25	100/25
Shallow donor density (cm^{-3})	$1.00x10^{20}$	$1.00x10^{5}$	0	$1.00x10^{17}$	0
Shallow acceptor density (cm^{-3})	0	0	$2.00x10^{16}$	0	$1.0x10^{17}$
Thickness (nm)	100	100	500	variable	2000

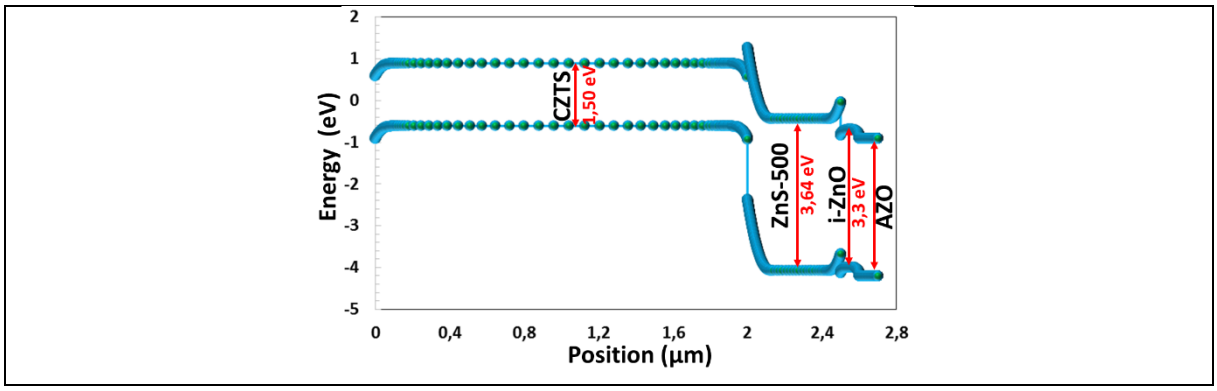

Figure 4. The band gap diagram of CZTS/ZnS-500 heterojunction solar cell

Since ZnS-500 thin film is more suitable for *n*-type buffer layer in terms of optical properties, the band diagram of solar cell modelled with this semiconductor is shown in the Figure 4. The spike like conduction band offset (CBO) is visible in the diagram of the heterojunction. Electrons in the conduction band of CZTS are prevented from moving to the conduction band of ZnS are blocked by the spike like CBO and may undergo recombination. This limits the charge accumulation in the depletion region. However, the holes in the ZnS valence band easily transition to the valence band of CZTS, which contributes to the charge accumulation.

3.1. The effect of the shallow donor density (N_D) in ZnS thin films on the PV performance of the CZTS/ZnS solar cells

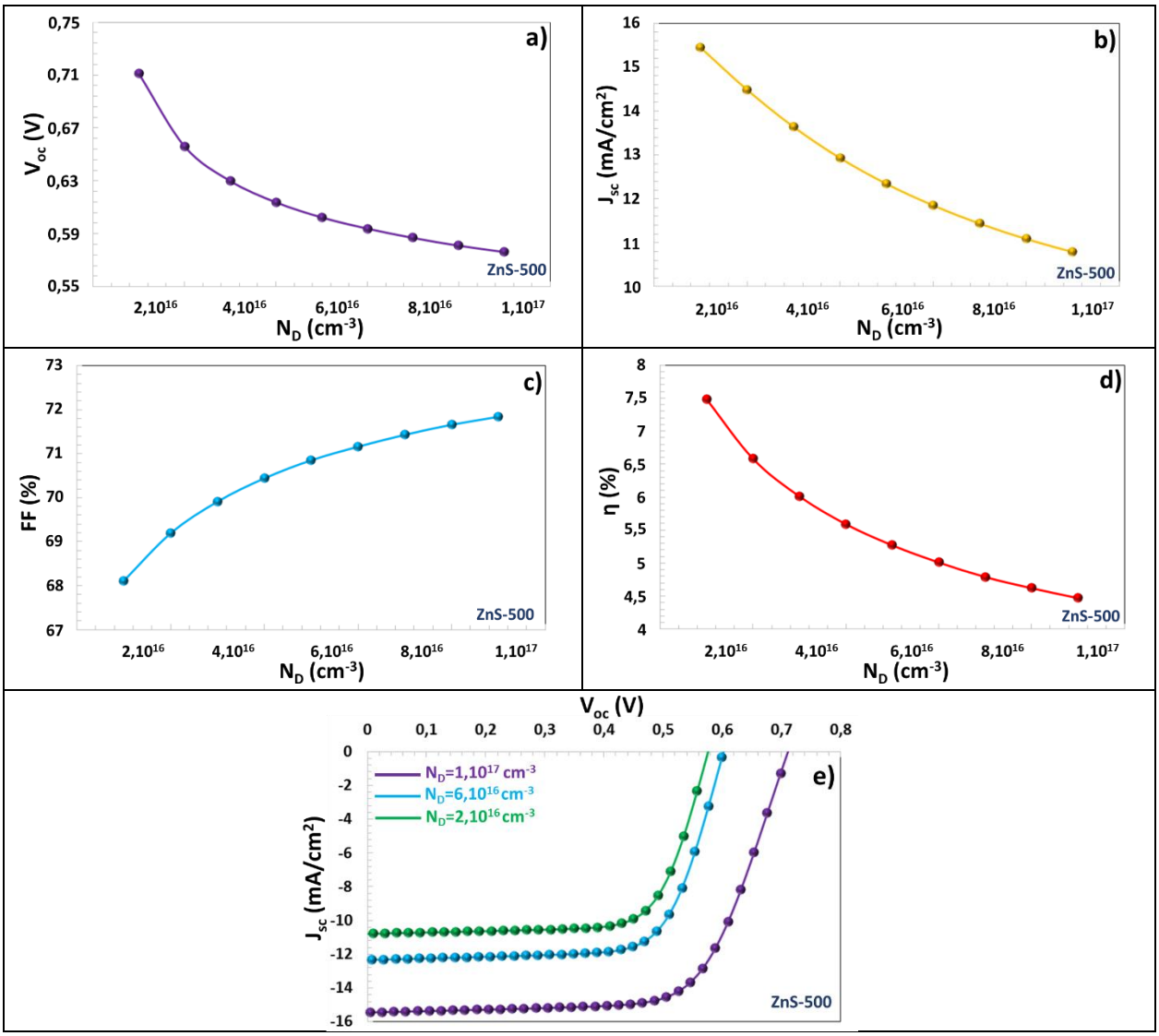

Figure 5. (a-d)The characteristics of the photovoltaic parameters vs N_D shallow donor density, e) $J-V$ characteristic for ZnS-500/CZTS solar cell

For ZnS-500/CZTS solar cell, with the increase of N_D , V_{OC}, J_{SC} and η decreased while FF increased, according to the characteristics in the Figure 5. Increasing N_D can lead to the formation of traps that act as recombination points for electrons and holes and the doping effect[35-37]. A high N_D value may cause doping into the depletion region. This doping causes the width of the depletion region to increase and the electrical field to decrease. The low electric field reduces the separation of electron and hole charges. This enhances the recombination of charges at the depletion site. Therefore, for ZnS-500/CZTS heterojunction solar cell, by increasing the N_D value from 2.10^{16} to 1.10^{17} cm^{-3}, V_{OC}, J_{SC} and η values, which decreased from 0.711 V to 0.576 V, from 15.44 mA/cm^2 to 10.78 mA/cm^2, from 7.48% to 4.47%, respectively [35]. However, FF value increment from 68.11% to 71.84%, which attributed a higher maximum power point.

Table 2. The photovoltaic parameters of CZTS/ZnS-500 heterojunction solar cell on N_D shallow donor density

N_D (cm^{-3})	V_{OC}(V)	J_{SC}(mA/cm^2)	FF (%)	η (%)
2.10^{16}	0.711	15.44	68.11	7.48
3.10^{16}	0.656	14.48	69.19	6.58
4.10^{16}	0.629	13.64	69.91	6.01
5.10^{16}	0.613	12.92	70.44	5.59
6.10^{16}	0.602	12.34	70.85	5.27
7.10^{16}	0.593	11.84	71.16	5.01
8.10^{16}	0.586	11.436	71.43	4.79
9.10^{16}	0.581	11.086	71.66	4.62
1.10^{17}	0.576	10.78	71.84	4.47

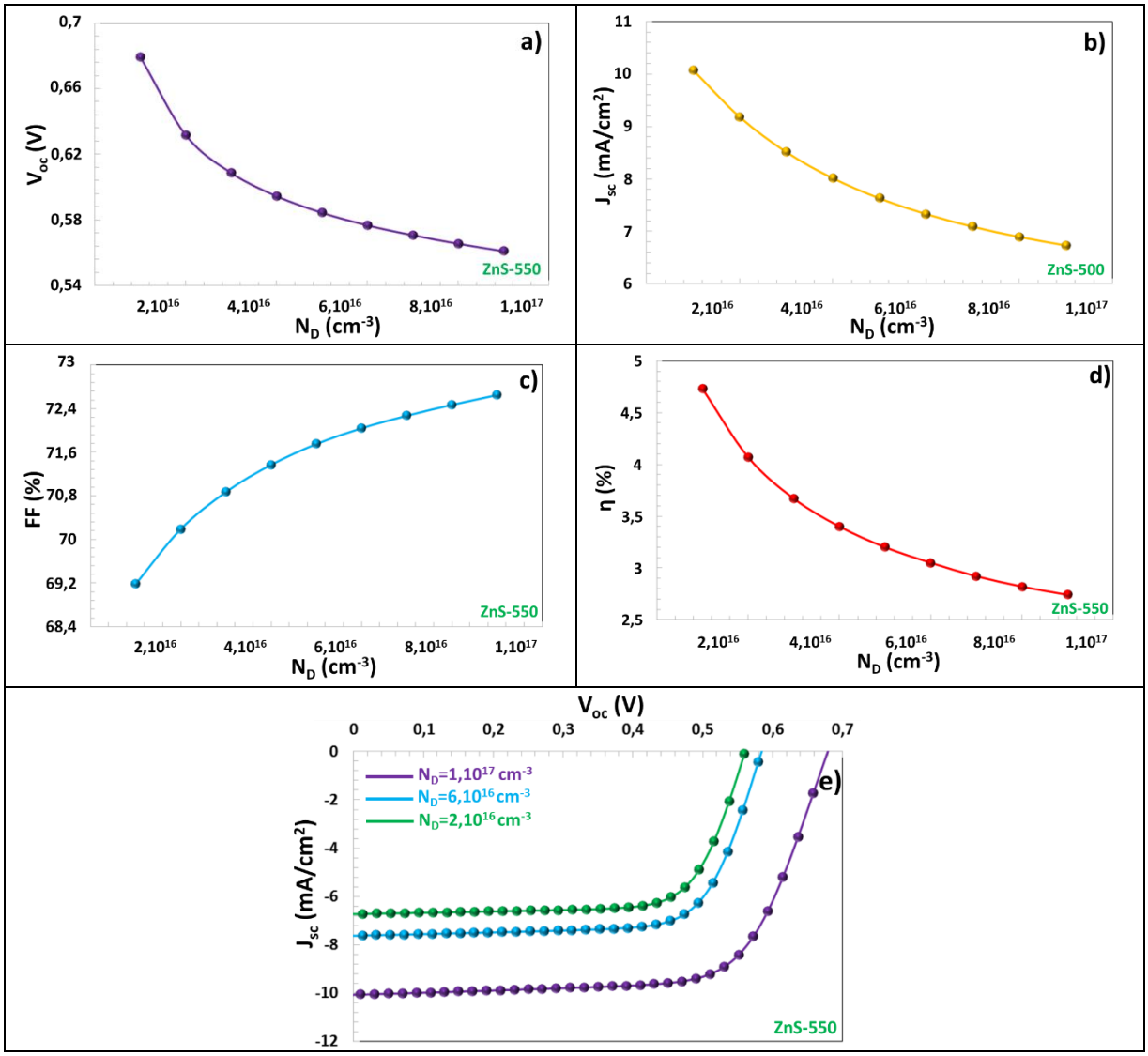

Figure 6. (a-d)The characteristics of the photovoltaic parameters vs N_D shallow donor density, e) $J-V$ characteristic for ZnS-550/CZTS solar cell

For ZnS-500/CZTS heterojunction solar cell, by increasing the N_D value from 2.10^{16} to 1.10^{17} cm^{-3}, V_{OC}, J_{SC} and η values, which decreased from 0.679 V to 0.560 V, from 10.07 mA/cm^2 to 6.73 mA/cm^2, from 4.73 % to 2.74 %, respectively. FF value increased from 69.18 % to 72.27 %. Since ZnS-550

thin film absorbs more photons compared to ZnS-500, it limits light penetration into the CZTS absorber layer. Thus, in the active layer, less photo-excited charge carriers are formed compared to ZnS-500/CZTS a solar cell. This causes the photocurrent, J_{SC} and V_{OC} values to decrease.

Table 3. The photovoltaic parameters of CZTS/ZnS-550 heterojunction solar cell on N_D shallow donor density

N_D (cm^{-3})	V_{OC}(V)	J_{SC}(mA/cm^2)	FF (%)	η (%)
2.10^{16}	0.679	10.07	69.18	4.73
3.10^{16}	0.631	9.18	70.19	4.07
4.10^{16}	0.608	8.51	70.87	3.67
5.10^{16}	0.594	8.01	71.37	3.4
6.10^{16}	0.584	7.62	71.75	3.2
7.10^{16}	0.576	7.33	72.04	3.05
8.10^{16}	0.570	7.09	72.27	2.92
9.10^{16}	0.565	6.89	72.47	2.82
1.10^{17}	0.560	6.73	72.65	2.74

CONCLUSIONS:

The extinction coefficient of ZnS-550 thin film is higher than the others, while its skin depth is lower. The solar cell consisting of Au/CZTS/ZnS-500&ZnS-550/i-ZnO/AZO layers was modelled with the SCAPS-1D program. The increase on N_D in ZnS thin films causes doping and reduction of the electric field in the depilation region, thus deteriorating the photovoltaic performance. For ZnS-500/CZTS heterojunction solar cell, by increasing the N_D value from 2.10^{16} to 1.10^{17} cm^{-3}, V_{OC}, J_{SC} and η values, which decreased from 0.679 V to 0.560 V, from 10.07 mA/cm^2 to 6.73 mA/cm^2, from 4.73 % to 2.74 %, respectively. FF value increased from 69.18 % to 72.27 %. Since ZnS-550 thin film absorbs more photons compared to ZnS-500, it limits light penetration into the CZTS absorber layer. The SnO_2 intermediate layer limits recombination by passivating the interfacial states between the CZTS and ZnS semiconductors. Thus, there is a significant enhance in the voltage and power conversion efficiency of the solar cell.

Acknowledgements

Authors would kindly like to thank to

- Selcuk University, Scientific Research Projects (BAP) Coordination Office for the support with the number 15201070 and 19401140 projects,
- Selçuk University, High Technology Research and Application Center (İL-TEK) and
- SULTAN Center for infrastructures

Dr. Marc Burgelman's group, University of Gent, Belgium for providing permission for us to use SCAPS-1D simulation program

Reference

1. GREENY, M.A., et al., *Solar cell efficiency tables (version 37).* Progress in photovoltaics (Print), 2011. **19**(1): p. 84-92.
2. Noufi, R. and K. Zweibel. *High-efficiency CdTe and CIGS thin-film solar cells: highlights and challenges*. in *2006 IEEE 4th World Conference on Photovoltaic Energy Conference*. 2006. IEEE.
3. Cui, X., et al., *Cd-Free Cu 2 ZnSnS 4 solar cell with an efficiency greater than 10% enabled by Al 2 O 3 passivation layers.* Energy & environmental science, 2019. **12**(9): p. 2751-2764.
4. Green, M., et al., *Solar cell efficiency tables (version 57).* Progress in photovoltaics: research and applications, 2021. **29**(1): p. 3-15.
5. Lee, S., et al., *Effect of annealing treatment on CdS/CIGS thin film solar cells depending on different CdS deposition temperatures.* Solar Energy Materials and Solar Cells, 2015. **141**: p. 299-308.
6. Nykyruy, L., et al., *Evaluation of CdS/CdTe thin film solar cells: SCAPS thickness simulation and analysis of optical properties.* Optical Materials, 2019. **92**: p. 319-329.
7. Nguyen, M., et al., *ZnS buffer layer for Cu2ZnSn (SSe) 4 monograin layer solar cell.* Solar Energy, 2015. **111**: p. 344-349.
8. Kim, J., et al., *Optimization of sputtered ZnS buffer for Cu2ZnSnS4 thin film solar cells.* Thin Solid Films, 2014. **566**: p. 88-92.
9. Olopade, M., O. Oyebola, and B. Adeleke, *Investigation of some materials as buffer layer in copper zinc tin sulphide (Cu2ZnSnS4) solar cells by*

SCAPS-1D. Advances in Applied Science Research, 2012. **3**(6): p. 3396-3400.
10. Vasekar, P.S. and T.P. Dhakal, *Thin film solar cells using earth-abundant materials.* Solar Cells-Research and Application Perspectives, 2013: p. 145-168.
11. Shin, B., et al., *Thin film solar cell with 8.4% power conversion efficiency using an earth-abundant Cu2ZnSnS4 absorber.* Progress in Photovoltaics: Research and Applications, 2013. **21**(1): p. 72-76.
12. Wangperawong, A., et al., *Aqueous bath process for deposition of Cu2ZnSnS4 photovoltaic absorbers.* Thin Solid Films, 2011. **519**(8): p. 2488-2492.
13. Zhao, W., W. Zhou, and X. Miao. *Numerical simulation of CZTS thin film solar cell*. in *2012 7th IEEE International Conference on Nano/Micro Engineered and Molecular Systems (NEMS)*. 2012. IEEE.
14. Ben Nasr, T., et al., *Effect of pH on the properties of ZnS thin films grown by chemical bath deposition.* Thin Solid Films, 2006. **500**(1): p. 4-8.
15. Bioki, H.A. and M.B. Zarandi, *Effects of annealing and thickness on the structural and optical properties of crystalline ZnS thin films prepared by PVD method.* International Journal of Optics and Photonics, 2011. **5**(2): p. 121-127.
16. Gilbert, B., et al., *X-ray absorption spectroscopy of the cubic and hexagonal polytypes of zinc sulfide.* Physical Review B, 2002. **66**(24): p. 245205.
17. Hathot, S.F., et al., *Influence of deposition time on absorption and electrical characteristics of ZnS thin films.* Optik, 2022. **260**: p. 169056.
18. Abdi, F. and H. Savaloni, *Investigation of the growth conditions on the nano-structure and electrical properties of ZnS chiral sculptured thin films.* Applied Surface Science, 2015. **330**: p. 74-84.
19. Zakerian, F. and H. Kafashan, *Investigation the effect of annealing parameters on the physical properties of electrodeposited ZnS thin films.* Superlattices and Microstructures, 2018. **124**: p. 92-106.
20. Kodigala, S.R., *Thin film solar cells from earth abundant materials: growth and characterization of Cu2 (ZnSn)(SSe) 4 thin films and their solar cells*. 2013: Newnes.
21. Li, J., et al., *Manipulating the morphology of CdS/Sb2S3 heterojunction using a Mg-doped tin oxide buffer layer for highly efficient solar cells.* Journal of Energy Chemistry, 2022. **66**: p. 374-381.
22. Liu, J., et al., *Thermal Evaporation–Deposited Hexagonal CDS Buffer Layer to Boost Performance of Sb2 (S, Se) 3 Solar Cells.* Available at SSRN 4030312.
23. Sreejith, M., et al., *Tuning the properties of sprayed CuZnS films for fabrication of solar cell.* Applied physics letters, 2014. **105**(20): p. 202107.
24. El-Hagary, M., et al., *Effect of γ-irradiation exposure on optical properties of chalcogenide glasses Se70S30− xSbx thin films.* Radiation Physics and Chemistry, 2012. **81**(10): p. 1572-1577.
25. Chabou, N., et al., *Deposition time and annealing effects on morphological and optical properties of ZnS thin films prepared by chemical bath deposition.* Materials Science-Poland, 2019. **37**(3): p. 404-416.
26. Akaltun, Y., et al., *The relationship between refractive index-energy gap and the film thickness effect on the characteristic parameters of CdSe thin films.* Optics Communications, 2011. **284**(9): p. 2307-2311.
27. Ravindra, N., P. Ganapathy, and J. Choi, *Energy gap–refractive index relations in semiconductors–An overview.* Infrared physics & technology, 2007. **50**(1): p. 21-29.
28. Yiğit Gezgin, S. and H.Ş. Kiliç, *The effect of Ag plasmonic nanoparticles on the efficiency of CZTS solar cell: an experimental investigation and numerical modelling.* Indian Journal of Physics, 2023. **97**(3): p. 779-796.
29. Gezgin, S.Y., *Modelling and investigation of the electrical properties of CIGS/n-Si heterojunction solar cells.* Optical Materials, 2022. **131**: p. 112738.
30. Houimi, A., S. Yiğit Gezgin, and H.Ş. Kılıç, *Theoretical Analysis of Solar Cell Performance with Different Backsurface-Filed Layers Utilizing Experimental Results of CdS Films Deposited by Pulsed Laser*. physica status solidi (a), 2022. **219**(11): p. 2100780.
31. Benami, A., *Effect of CZTS parameters on photovoltaic solar cell from numerical simulation.* J. Energy Power Eng, 2019. **13**(1).
32. Adewoyin, A.D., et al., *Development of CZTGS/CZTS tandem thin film solar cell using SCAPS-1D.* Optik, 2019. **176**: p. 132-142.
33. AlZoubi, T. and M. Moustafa, *Numerical optimization of absorber and CdS buffer layers in CIGS solar cells using SCAPS.* Int. J. Smart Grid Clean Energy, 2019. **8**: p. 291-298.
34. Shukla, V. and G. Panda, *The performance study of CdTe/CdS/SnO2 solar cell.* Materials Today: Proceedings, 2020. **26**: p. 487-491.
35. Meher, S., L. Balakrishnan, and Z. Alex, *Analysis of Cu2ZnSnS4/CdS based photovoltaic cell: a numerical simulation approach.* Superlattices and Microstructures, 2016. **100**: p. 703-722.
36. Gupta, G.K. and A. Dixit, *Simulation studies of CZT (S, Se) single and tandem junction solar cells towards possibilities for higher efficiencies up to 22%.* arXiv preprint arXiv:1801.08498, 2018.
37. Zhang, H., et al., *Prospects of Zn (O, S) as an alternative buffer layer for Cu2ZnSnS4 thin-film solar cells from numerical simulation.* Micro & nano letters, 2016. **11**(7): p. 386-390.